Application of Scanning Electron Microscopy to X-ray Analysis of Frozen-hydrated Sections II. Analysis of Standard Solutions and Artificial Electrolyte Gradients

ALBERT J. SAUBERMANN, REINIER BEEUWKES III, and PATRICIA D. PETERS
Department of Anaesthesia, Harvard Medical School at Beth Israel Hospital and the C. Dana Research Institute, Boston, Massachusetts 02215, and Department of Physiology, Harvard Medical School, Boston, Massachusetts 02215

ABSTRACT New specimen handling and analytic techniques for the application of x-ray microanalysis to studies of cell and organ biology have been recently described (Saubermann et al., 1981, *J. Cell Biol.* 88:257–267). Based on these techniques, absolute quantitative standardization has been established through x-ray analysis of frozen-hydrated and then dried sections of independently measured standard solutions of elements. These experiments demonstrate that the specific techniques employed have a probable error of <10%. Artificial electrolyte gradients established in gelatin were subjected to analysis to determine whether there was elemental displacement under non-membrane-limited conditions at the temperatures employed for sectioning (−30° to −40°C). No significant difference was observed between such gradients in serial sections cut at −30° and −80°C. Similarly, no additional ice-crystal-damage artifact was found in sections cut at −30°C when compared with sections cut at −80°C. Thus, in terms of ice-crystal size, gradient maintenance, and compartmental differentiation, cryosectioning at −30° to −40°C was not associated with redistribution incompatible with 1- to 2-μm spatial resolution, and absolute measurements of elemental concentration were practical within regions of this size.

The application of x-ray microanalysis to studies of cell and organ physiology requires that the precision and accuracy of the specific specimen handling and analytic techniques employed be established. Although the validity of standard methods for the study of metal and mineral specimens has been long established (14, 23), assessment of the applicability of these techniques to biology is still in the early stages. Although several methodological approaches for biological analysis have been previously described (1, 3, 6–8, 12, 13, 15, 16, 19), no single method has become generally accepted. Recently a method has been described in detail for the direct x-ray analysis of frozen-hydrated sections. In development of that method, it was found that to obtain flat, 0.5-μm-thick sections having recognizable morphological compartments, it was necessary to perform cryosectioning at −40°C. Sectioning at this temperature might result in recrystallization of cell water or elemental redistribution. In addition, although the initial studies showed that distinct differences in elemental mass fractions could be detected in different compartments, the quantitative aspects of the technique were not established (16). We now report studies in which the methodology for x-ray analysis of frozen-hydrated sections is validated through analysis of frozen-hydrated standard solutions and artificial electrolyte gradients.

MATERIALS AND METHODS

The techniques employed for specimen handling in these studies have been previously described in detail (16). Specimens were shock-frozen in Freon 12 at its melting point (−158°C) and transferred to a cryochamber mounted on a microtome (MT-2B, Sorvall; Dupont Instruments, Sorvall Biomedical Div., Wilmington, Del.). The cooling system of the cryochamber was designed to surround the knife and specimen with a continuous flow of cold nitrogen gas. The nitrogen temperature was controlled to maintain the specimen at the desired temperature. Sections were cut by means of a steel razor-blade knife with accompanying retractable glass antiroll plate. The microtome was set at 0.5-μm thickness, and sections were mounted on a specimen holder within the cooled microtome

THE JOURNAL OF CELL BIOLOGY · VOLUME 88 FEBRUARY 1981 268–273

chamber (16). The specimen holder was transferred to a liquid nitrogen–cooled stage (−175°C) in the vacuum column of the scanning microscope (AMR 900; AMRay Corp., Burlington, Mass.), using a simple transfer system consisting of a cooled copper sink in a sealable Delrin cylinder (16). Spectra were obtained with an energy-dispersive x-ray analyzer (Kevex 5100 system with a 10-mm^2 155 eV Si(Li) detector; Kevex Corp., Foster City, Calif), and analyzed with an online minicomputer (PDP-11/03; Digital Equipment Corp., Maynard, Mass). A 30-keV accelerating voltage and a 0.1-nA probe current (measured with a Faraday cup attached to the microscope cold stage) were used for all measurements. The take-off angle was 35°C. X-ray spectra were obtained at 20 eV/channel during live counting times of 30–100 s.

Analytical Method

The Hall method of quantitative analysis was employed (9). This method determines relative mass fraction (R-value) from the ratio of characteristic counts to continuum. Comparison of R-values obtained from unknowns and standards allows absolute standardization. R-values were calculated by subtracting background counts (b_x) from the characteristic x-ray counts for each element (P_x) and dividing this net counting rate by counting rate in a selected portion of the continuum (W_T) corrected for extraneous continuum counts contributed by the supporting film and holder (W_E):

$$R\text{-}value_x = \frac{P_x - b_x}{W_T - W_E}. \quad (1)$$

The validity of this general method has been extensively documented (8, 9, 18, 21).

Characteristic x-rays of elements of interest were measured within the following fixed keV ranges: sodium, 0.96–1.12 keV; phosphorus, 1.92–2.08 keV; sulfur, 2.24–2.40 keV; chlorine, 2.52–2.68 keV; potassium, 3.24–3.40 keV; calcium, 3.60–3.76 keV; and iodine, 3.84–4.06 keV. Continuum counts were recorded within the energy range of 4.60–6.00 keV inclusive. Background radiation was subtracted from the spectrum by using a "top hat" digital band-pass filter (20) technique having the following configuration:

$$C'(I) = \sum_{I-3}^{I+3} C(I)/7 - \left[\sum_{I+4}^{I+7} C(I) + \sum_{I-4}^{I-7} C(I)\right]/8, \quad (2)$$

where $C(I)$ is the number of counts in the Ith channel of the original spectrum at 20 eV/channel resolution. Net counting rate for element x was given by:

$$P_x - b_x = \sum_{I_L}^{I_L+I_H} C'(I), \quad (3)$$

where I_L is the lowest channel, and I_H is the highest channel of the energy region for element x. Application of this function was done online, using a relatively simple interactive Fortran IV program.[1]

The effect of this signal processing was to suppress channel-to-channel high-frequency variations (smoothing function), and to remove low-frequency background. Thus use of this filter produced a new spectrum with a background equal to zero (Fig. 1). "Negative" counts introduced by the filtering process on either side of the peaks were defined as zero before integration of the counts for that characteristic element (Fig. 1). Corrections for extraneous or escape peaks were unnecessary, as there were no extraneous characteristic x-rays or escape peaks in the spectra. Potassium K_β characteristic x-ray counts within the calcium energy range were estimated from the measured overlap of K and Ca characteristic peaks and subtracted from the calcium net count rate after filtering.

The weight fraction of water in specimens analyzed was calculated by use of two general methods. The first (A) was based upon the proportionality between continuum and total mass based upon the relative constancy of average atomic number in biological tissue (10): $\%\ water = [1 - (Continuum_{dried})/(Continuum_{hydrated})] \times 100\%$. The second method ($B$) was based upon the change in weight fraction (R-value) with drying of an element normally present in the section (the element usually chosen was potassium, although the proportional change in R-value with drying was similar for each element in the hydrated specimen): $\%\ water = [1 - (R\text{-}value_{x,\ hydrated})/(R\text{-}value_{x,\ dried})] \times 100\%$.

Standard Curves

Na, P, S, Cl, K, and Ca standards were prepared by adding 2.0 gm of previously dialyzed polyvinyl pyrrolidone (40,000 mol wt PVP; Aldrich Chemical Co., Milwaukee, Wisc.) to 8.0-cm^3 aliquots of standard solutions of NaCl, KSCN, KH_2PO_4, and $CaCl_2$. The K and Na concentrations in each solution were determined by flame photometry before the PVP was added. Ca standards were analyzed by atomic absorption spectrophotometry. The weight of each elemental standard was determined before and after drying (Fig. 2). These data were used as an independent measure of absolute weight fraction.

Droplets of each standard were placed on copper cylinders, which were immediately inverted and plunged into Freon 12 at its melting point. Frozen droplets were then sectioned at −40°C, and sections were analyzed in the frozen-hydrated state at −175°C. 20 × 20-μm areas were randomly chosen and were analyzed, using 90-s live counting times. The sections were then freeze-dried in the microscope by raising the stage temperature to −50°C for 45 min. The stage was then recooled to −175°C, and the sections were reanalyzed.

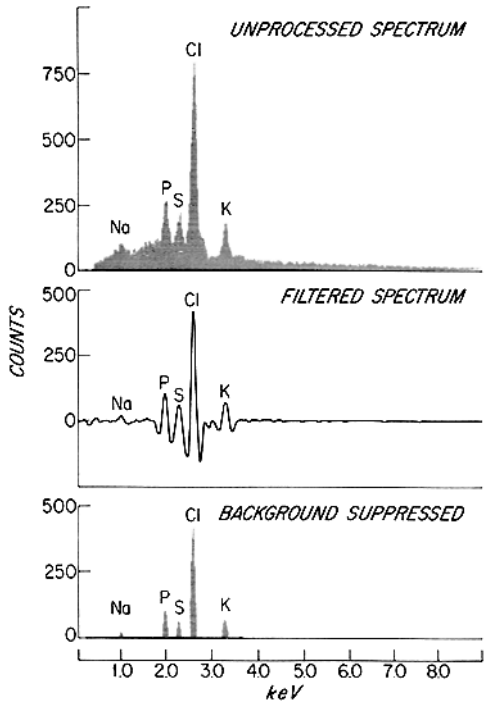

FIGURE 1 X-ray spectrum before and after signal processing. (Upper) In the original spectrum, elemental peaks rise above a mass proportional continuum (background signal). (Middle) Application of the digital band-pass filter employed in this study suppressed background counts by selectively eliminating the channel-to-channel count variations (high-frequency variation) and the slowly changing continuum counts (low-frequency variation). (Lower) Setting the baseline of the processed spectrum to zero suppresses the background and yields clearly defined elemental peaks.

Ice-crystal-damage Artifacts

Drops of 20% bovine serum albumin solution were placed on copper cylinders, which were then inverted and plunged into melting Freon 12. Sections (0.5-μm thick) were then cut at a very low temperature (−80°C), transferred, checked for hydration, and permitted to freeze-dry as described above. The stage was then recooled to −175°C, and the sections were examined and photographed in the STEM mode at a magnification of ×5,000. Meanwhile, droplets remaining in the microtome were warmed to −30°C and maintained at that temperature for 2 h. Several sections were then cut and discarded, after which a second group of two or three sections was then cut at −30°C from each droplet previously examined and transferred to the microscope. The sections were checked for hydration, freeze-dried, examined, and photographed as before. The size of ice-crystal-damage artifacts was determined by a random sampling technique. Micrographs were enlarged and a line approximately bisecting the section image and perpendicular to the surface of the section was drawn. The dimension parallel to the line was measured for each ice-crystal-damage artifact lying within 10 μm of the edge of the section and touching the line.

Electrolyte Diffusion

Artificial electrolyte gradients were formed in gelatin blocks by diffusion. Gelatin solutions were prepared by placing 15 grams of gelatin (Knox) in 30 ml of distilled water in an Erlenmeyer flask. To dissolve the gelatin, sealed flasks

[1] A copy of this program is available from the authors upon request.

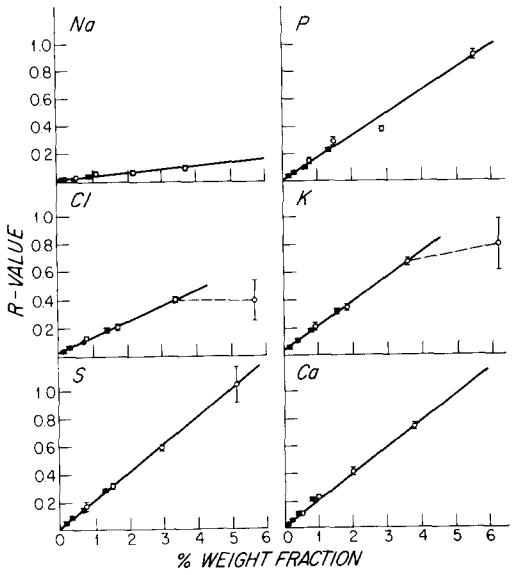

FIGURE 2 Standard curves obtained during x-ray microanalysis of frozen-hydrated (closed circles) and frozen-dried (open circles) sections cut from frozen droplets of standard solutions. Each point represents the mean of six determinations ± standard deviation. In the physiological range, R-value for each element increased as a linear function of the measured weight fraction (Na, $r = 0.9332$; Cl, $r = 0.9934$; S, $r = 0.9979$; P, $r = 0.9811$; K, $r = 0.9972$; Ca, $r = 0.9961$).

were intermittently agitated during a 4-h period at 80°C. When the gelatin was fully dissolved it was poured into warm (80°C) glass petri dishes, sealed with Parafilm, and placed in a refrigerator at 4°C to gel. Cylinders of solidified gel, 1 cm in diameter and ~5-mm high, were cut with a cleaned cork borer. A solution of 15% NaCl, 15% KI, colored green with food coloring (Durkee, SCM Corp., Cleveland, Ohio), was placed on the gel surface and left for 1 min. The unabsorbed solution was then removed by absorption with filter paper and the gel cylinders were then quickly frozen in melting Freon 12. Small pieces, suitable for mounting in the microtome chuck, were chipped from the frozen gel cylinder under LN_2, using a cooled razor blade. Sections (0.5-μm thick) were then cut at −80°C with the specimen holder rotated so that the green surface was at the top edge. The green dye representing the diffusion front was uniformly parallel to the surface and was visible to a depth of ~1 mm.

Sections were then transferred to the microscope for analysis. To define the gradients, analysis was performed at five locations. A 20- × 20-μm raster was first positioned with its edge a measured distance from the surface and then at 60-μm intervals of depth (total section width was ~0.5 mm). After initial analysis, the gel specimen remaining in the microtome was warmed to −30°C and maintained at that temperature for ~30 min. Several sections were cut and discarded, after which a section was cut and transferred, and the gradient was reanalyzed.

RESULTS

Analytical Method and Standards

Continuum counting rates were between 30 and 300 counts/s depending upon thickness, hydration, and composition. There were no characteristic peaks in the continuum energy range. Continuum arising from specimen support film and other sources was generated at a rate of between 6 and 12 counts/s, depending primarily upon support-film thickness. Thus the correction factor for continuum was usually between 3 and 8% of specimen continuum (hydrated). Instrumental electronic drift in the energy-dispersive x-ray detection system resulted in only small shifts (2–3 eV) in peak centroids. The error introduced by this variability was <1% of the measured value (Fig. 3).

90% of all sections transferred were judged suitable for analysis by previously described criteria (16). The data reported was derived from analysis of all standard sections that met the criteria. The relative mass fractions (R-value) for Na, P, S, Cl, K, and Ca were found to be linear functions of the independently measured absolute weight fraction of each element over the concentration range studied (Fig. 2). This relationship deviated from linearity for potassium and chlorine above a weight fraction of 3%. Linearity was found in analysis of both hydrated and dried groups of standards. Drying resulted in an increase in both absolute mass fraction and measured R-value so that measurements made on a single standard in both hydrated and dried states could be plotted on the same R-value vs. mass fraction curve. Standard deviations of measured R-values (obtained from multiple measurements of standard solutions) ranged between 3 and 9% of the mean value measured (Fig. 2).

As a test of absolute standardization, the R-value standard curve derived from the analysis of frozen-hydrated and dried sections of standard KSCN solutions was used to determine the absolute weight fraction of K in frozen hydrated sections cut from KH_2PO_4 standard solutions. The result of this determination is shown in Table I. Differences between actual and measured weight fraction were <5% (range, 0.2–4.6%) for K concentrations up to 470 mM. The potassium K_β characteristic x-ray counts within the calcium energy range were found to be a linear function ($r = .990$) of total potassium K_α counts after filtering (Fig. 4). Thus calcium could be analyzed in the presence of potassium. However, this simple peak-overlap separation technique was applicable only to samples in which the calcium/potassium ratio was >0.2.

The weight fraction of water as determined by x-ray microanalysis was compared to the weight fraction measured gravimetrically (Table II). Water fraction as measured by ratio of hydrated R-value to dried R-value (method *B* above) was found to be within 4% (range, 0.2–3.7%) of that determined gravimetrically. Calculation of water fraction from continuum ratio (method *A*) was less accurate (range, 3.9–14.4% difference).

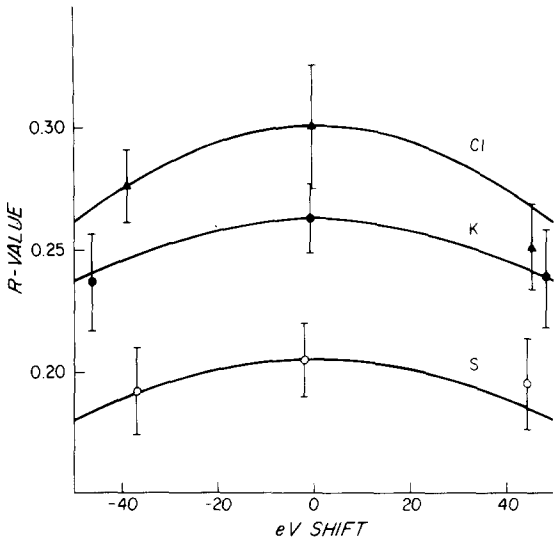

FIGURE 3 Changes in Cl (2.62 keV), K (3.31 keV), and S (2.31 keV) R-values (±SD) observed when the calculated peak centroids were shifted above (positive shift) or below (negative shift) their theoretical centroids. Solid lines show predicted shifts in R-value for each element as their centroid was shifted negatively or positively. Calibration of the pulse processor kept actual centroid shifts within ±5 eV of theoretical centroids, thus keeping this source of error in calculated R-values to <1%.

TABLE I

Measurement of K Concentration by X-ray Microanalysis

Measured [K]	Actual [K]	Mean % difference
mm/kg	*mm/kg*	
51.3 ± 7.9	49.4	3.8
94.3 ± 4.1	98.8	4.6
235.7 ± 25.0	235.2	0.2
460.2 ± 43.8	470.2	2.1

Standard solutions in KH_2PO_4 were analyzed in bulk by flame photometer and in sections by x-ray microanalysis based upon the standard curves obtained by analysis of KSCN solution (Fig. 2). Concentrations (mm/kg ± SD, $n = 6$) are shown. The two lowest concentrations were measured in hydrated sections, the two highest were measured in the same sections after drying.

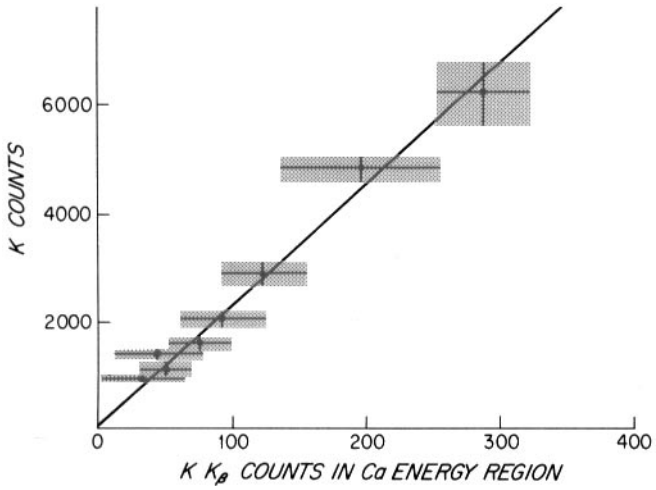

FIGURE 4 Potassium K_β characteristic x-ray counts within the calcium energy range. Such counts were found to be a linear function ($r = .990$) of total potassium K_α counts after filtering. The standard deviations of mean K_α counts (vertical bar) and of mean K_β counts within the calcium energy range (horizontal bar) are shown for each group of observations.

Ice-crystal-damage Artifacts

There was no measurable difference between the size of ice-crystal-damage artifacts in serial sections cut at −80°C and in the section cut after equilibration at −30°C. The mean dimension of the ice-crystal-damage artifacts in −80°C sections was 0.40 ± 0.02 μm SD ($n = 47$), whereas in the −30°C sections the dimension was 0.42 ± 0.02 μm SD ($n = 51$).

Artificial Electrolyte Gradients

Artificial electrolyte gradients established by diffusion in gelatin blocks were subjected to five-point analysis. Best-fit exponential curves were calculated by computer for each element in gradients sectioned at each temperature (Fig. 5). The observations made were tested for significant differences attributable to temperature over the range of observation by two methods: covariance analysis of the linearized (semilog) data pairs; and by comparison of the pooled residual sums of squares to the total residual sums of squares associated with the non-transformed data pairs fitted to a single exponential function. This statistical analysis showed no significant difference between the electrolyte gradients measured in sections cut at −80°C and those measured in −30°C sections. Regression coefficients for the best-fit curves for the combined gradients were $r = .9792$ (Na), $r = .9924$ (Cl), $r = .9813$ (K), and $r = .9888$ (I).

DISCUSSION

A recent study of techniques for producing, handling, and analyzing frozen-hydrated 0.5-μm-thick sections of biological tissue for x-ray microanalysis found that cryosectioning temperatures in the range of −30°C to −50°C were required to reduce specimen brittleness and minimize sectioning work (16). Although that study showed that qualitative measurements were possible in sections cut at such temperatures, it has been proposed that cryosectioning at much lower temperatures (below −80°C) is mandatory to prevent elemental displacement resulting from ice recrystallization, ice-crystal growth, and transient melting. Thus Thornburg and Mengers (22) theorized, from pressure considerations, that cryosectioning at −50°C resulted in a layer of water several hundred angstroms thick being formed at the knife edge that quickly refroze as the knife edge advanced. On the other hand, Hodson and Marshall (11) have presented evidence against such melting. Appleton (1) has also suggested that elemental displacement may result from

TABLE II

Measurement of Water Fraction by X-ray Microanalysis

Sample wet weight	Water fraction, %				
	Gravimetry	Method *A*	% Diff.	Method *B*	% Diff.
mm K/kg					
409.6	76.0	72.5	4.6	75.1	1.2
194.7	77.8	68.1	12.5	74.9	3.7
96.4	79.0	82.1	3.9	79.6	0.2
45.4	79.6	68.1	14.4	78.3	1.6

Standard solutions of KH_2PO_4 were analyzed in bulk by gravimetry and in sections by x-ray microanalysis, using two methods. Method *A* compared continuum from hydrated and dried sections. Method *B* compared R-values for potassium as measured in hydrated and dried sections. Each percentage represents a single determination based on a mean of six continuum or R-value measurements made in the hydrated state and six such measurements made in the same section after drying.

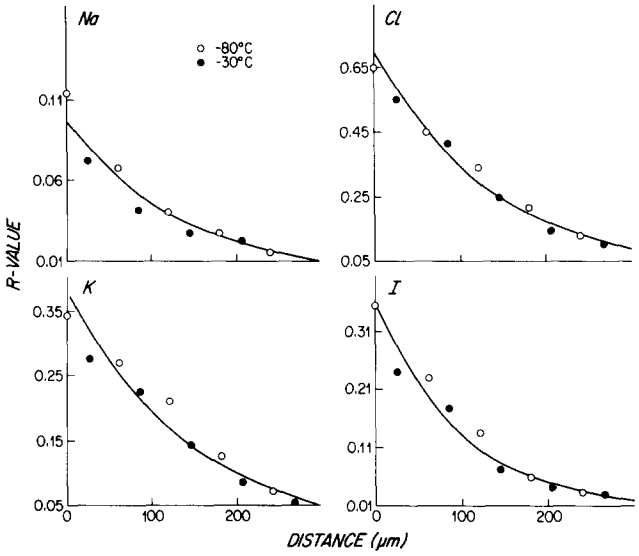

FIGURE 5 Observations and calculated best-fit exponential curves obtained by x-ray microanalysis of artificial electrolyte gradients. Gradients (Na, Cl, K, I) were established in gelatin blocks and were subjected to analysis in serial sections cut first at −80°C (○) and then at −30°C (●). Statistical analysis showed no significant difference between the electrolyte gradients observed in sections cut at these two temperatures.

cryosectioning. The present study thus sought to determine whether measurable elemental displacement occurred during cryosectioning at temperatures as warm as −30°C and to determine the accuracy and precision with which the concentration of diffusible elements could be defined in sections cut at such temperatures.

Analysis of Standards

The Hall method of quantitative analysis has been well documented (4, 8, 9, 18). It appears to be the most useful quantitative approach available for "thin"-section x-ray microanalysis of biological material. This method defines an R-value that is theoretically proportional to the mass fraction of an element in the region analyzed. Analysis of 0.5-μm sections of frozen standard solutions demonstrated a consistent linear relationship between measured R-value and independently determined weight fractions in both hydrated and dried sections over the range of concentrations commonly found in biological specimens. Furthermore, there was good agreement between measured concentrations and the known concentrations of solutes in standard solutions. The standard deviation of repeated measurements made in a single area was <10% (range, 3–9%). Given the fact that the method is applicable to tissue volumes $<10^{-12}$ liters in size, this precision is probably sufficient for many experiments in cell biology.

The standard deviation measured exceeded that expected from counting statistics alone. Such additional variation arose from three sources: instrumental shifts, measurement of characteristic peaks, and measurement of continuum. Instrumental shifts in peak centroids could result in significant error in quantitation. Use of the digital filter for background suppression made the characteristic x-ray peaks more sensitive to centroid shifts, requiring that careful attention be paid to pulse-processor calibration. A ±5-eV difference between actual and expected centroid location was accepted, as such a difference was found, on both theoretical and experimental grounds, to change R-values by <1%.

Potential sources of variation in measurement of characteristic peaks arose from three major sources. First, differential absorption of x-rays within the specimen; second, overlap of peaks; and third, the filtering process. X-rays having low energies tend to be preferentially absorbed within the specimen as the total solute concentration increases. Such differential absorption was not apparent in these studies. Peak overlap was minimized by the care taken to remove extraneous interfering characteristic elemental peaks through use of beryllium holders and carbon support films. Hence no extraneous spectral peak stripping was required, thus greatly simplifying the data reduction. However, the naturally occurring overlap of potassium K_β and calcium K_α x-rays, combined with the naturally low concentration of calcium in most tissue, makes the measurement of intracellular calcium difficult. Variation introduced by the digital filter changes the shape of characteristic peaks by making those peaks narrower and reducing the net integrated count rate. However, because in the standardization procedure the peaks of measured standards were similarly modified, the change in absolute peak amplitudes were relatively unimportant.

The variance of a measurement of the continuum is defined by Poisson counting statistics. However, the continuum counting rate used for calculation of R-value was corrected for extraneous continuum counts originating from the support film and specimen holder. Because such extraneous continuum could not be directly measured from the supporting film under the specimen, this correction probably introduced significant error. The efforts taken to minimize extraneous continuum generation reduced the magnitude of this correction to <10%. Thus if the actual extraneous contribution from film and holder under the region of analyzed tissue were within a factor of two of that estimated, the accuracy of elemental mass fraction estimates would be 10%. Given the many sources of variance, the finding of a 10% probable error in any single determination must be considered satisfactory. This finding is consistent with the performance estimate of 10% reported by Shuman et al. (18). However, because the sources of variance can be identified, further improvement appears possible.

Weight Fraction of Water

In this study, water content was determined by two methods. The most direct, method *A*, compared continuum counts (proportional to total mass) from a region in the hydrated state with that measured in the dried state. Accuracy of this method depends upon the amount of tissue shrinkage. In tissue sections, reported linear shrinkage does not exceed 6% (15). The linear shrinkage of the standard solutions used here ranged from 5 to 15%. Such shrinkage would lead to underestimation of local water content. The second method (method *B*), compared R-values (weight fractions) measured for a single element in the same region before and after drying. These methods have been reported by Gupta et al. (8). The accuracy of method *B* is theoretically unaffected by tissue shrinkage and is relatively insensitive to fluctuations in probe current and instrumental drift. These theoretical advantages were demonstrated in the present studies. The error of the R-value method (method *B*) was one-third that of the continuum method (method *A*). The ability to measure local water fraction size in addition to local elemental levels is of great potential value to cell biologists because it permits local concentrations of elements to be defined as mass per unit water. Hence this approach may permit estimation of local molar concentration (millimoles per liter) in defined tissue compartments. Such estimations must, of course, be based upon reasonable assumptions regarding binding and activity.

Elemental Redistribution

Elemental redistribution could occur during cryosectioning if sufficient heat were transferred to melt the section. In a previous study the actual amount of work done during cryosectioning was determined by direct measurement of cutting force (17). Cutting 0.5-μm-thick sections at −80°C required more work, therefore, more potential thermal input to the section than cutting 0.5-μm-thick sections at −30°C (17). Based on "worst case" assumptions, at −80°C there was sufficient energy input to melt sections, whereas at −30°C melting could not occur. Such experimental observations indicate that it is, in fact, "safer" to cryosection at −30°C than at −80°C.

Elemental redistribution resulting from such relatively warm temperatures might be reflected by changes in ice-crystal size or by the dissipation of elemental gradients. Comparison of sections cut from the same block, first at −80°C and then at −30°C, showed no evidence that sectioning at warmer temperatures significantly increased the dimension of ice-crystal-damage artifacts, even after a 2- to 3-h period at −30°C. This is consistent with Christensen's suggestion (5) that the high molecular weight solutes present in cells raised the recrystallization

temperature to the range warmer than −30°C. Because the volume of the ice crystal would roughly depend upon the third power of its dimension, an unmeasurably small increase in size might result in a significant change in volume. However, because the mean size of ice crystals (0.4 μm) was much smaller than the raster scans employed (2–20 μm), such changes in volume would not effect the results of quantitative analysis.

Elemental gradients within tissue are usually associated with the presence of membranes or other diffusion-limiting structures. In the present study, we sought to determine whether elemental gradients formed in the absence of limiting membranes were dissipated by the processes involved in cryosectioning and analysis. It was found that no difference existed between those gradients observed in sections cut and maintained at −80°C and those observed in sections cut and maintained at −30°C. Although these artificial gradients were long compared to cellular dimensions, they corresponded well to dimensions of interstitial regions in tissue, regions that lack defining membranes. Other studies, using the same method, have shown differences in mass fractions of diffusible elements (Na, Cl, K) within 1–2 μm on either side of cellular membranes in sections cut at −40°C (2). Thus in terms of ice-crystal artifact size, gradient maintainance, and compartmental differentiation, it appears that cryosectioning at −30° to −40°C is not associated with elemental redistribution incompatible with 1-2-μm spatial resolution, and that quantitative measurement of elemental concentration in such sections is both feasible and accurate.

The authors wish to thank Mr. William Riley for his expert technical assistance, and Dr. Bernard J. Ransil, of the Core Laboratory, Clinical Research Center, Beth Israel Hospital, for his assistance with statistical analysis of the electrolyte gradients.

This work was supported by National Institutes of Health (NIH) grants GM 15904, and AM 18249. Dr. Beeuwkes is the recipient of NIH RCDA AM 00224 and a grant from R. J. Reynolds Industries, Inc.

Received for publication 3 December 1979, and in revised form 21 July 1980

REFERENCES

1. Appleton, T. C. 1974. A cryostat approach to ultrathin "dry" frozen sections for electron microscopy: a morphological and x-ray analytical study. *J. Microsc. (Oxf.)*. 100:49–74.
2. Bulger, R. E., R. Beeuwkes III, and A. J. Saubermann. 1981. Application of scanning electron microscopy to x-ray analysis of frozen hydrated sections. III. Distribution of elements in the rat renal papilla. *J. Cell Biol.* 88:274–280.
3. Cameron, I. L., N. K. R. Smith, and T. B. Pool. 1979. Element concentration changes in mitotically active and postmitotic enterocytes: an x-ray microanalysis study. *J. Cell Biol.* 80:444–450.
4. Chandler, J. A. 1976. A method for preparing absolute standards for quantitative calibration and measurement of section thickness with x-ray microanalysis of biological ultrathin specimens in EMMA. *J. Microsc. (Oxf.)*. 106:291–302.
5. Christensen, A. K. 1972. Frozen thin sections of fresh tissue for electron microscopy, with a description of pancreas and liver. *J. Cell Biol.* 51:772–804.
6. Dörge, A., R. Rick, K. Gehring, J. Mason, and K. Thurau. 1975. Preparation and applicability of freeze-dried sections in the microprobe analysis of biological soft tissue. *J. Microsc. Biol. Cell.* 22:205–214.
7. Fuchs, W., and B. Lindemann. 1975. Electron beam x-ray microanalysis of frozen biological bulk specimens below 130K. *J. Microsc. Biol. Cell.* 22:227–232.
8. Gupta, B. L., T. A. Hall, and R. B. Moreton. 1977. Electron probe x-ray microanalysis. *In* Transport of Ions and Water in Animals. B. L. Gupta, R. B. Moreton, J. L. Oschman, and B. J. Wall, editors. Academic Press Inc. (London) Ltd., London. 83–143.
9. Hall, T. A., H. C. Anderson, and T. Appleton. 1973. The use of thin specimens for x-ray microanalysis in biology. *J. Microsc. (Oxf.)*. 99:177–182.
10. Hall, T. A., H. O. E. Rockert, and R. L. de C. H. Saunders. 1972. X-ray Microscopy in Clinical and Experimental Medicine. Charles C. Thomas, Publisher, Springfield, Ill. 227.
11. Hodson, S., and J. Marshall. 1972. Evidence against through-section thawing whilst cutting on the ultracryotome. *J. Microsc. (Oxf.)*. 95:459–465.
12. Hutchinson, T. E., M. Bacaner, J. Broadhurst, and J. Lilley. 1974. Instrumentation for direct microscopic elemental analysis of frozen biological tissue. *Rev. Sci. Instrum.* 45:252–255.
13. Ingram, F. D., M. J. Ingram, and C. A. M. Hogben. 1974. An analysis of the freeze dried, plastic embedded electron probe specimen preparation. *In* Microprobe Analysis as Applied to Cells and Tissues. T. Hall, P. Echlin, and R. Kaufmann, editors. Academic Press, Inc., New York. 119–146.
14. Reed, S. J. B. 1973. Principles of x-ray generation and quantitative analysis with the electron microprobe. *In* Microprobe Analysis. C. A. Andersen, editor. J. Wiley & Sons, New York. 53–81.
15. Saubermann, A. J., and P. Echlin. 1975. The preparation, examination and analysis of frozen hydrated tissue sections by scanning transmission electron microscopy and x-ray microanalysis. *J. Microsc. (Oxf.)*. 105:155–191.
16. Saubermann, A. J., P. Echlin, P. D. Peters, R. Beeuwkes. 1981. Application of scanning electron microscopy to x-ray analysis of frozen hydrated sections. I. Specimen handling techniques. *J. Cell Biol.* 88:257–267.
17. Saubermann, A. J., W. D. Riley, and R. Beeuwkes III. 1977. Cutting work in thick section cryomicrotomy. *J. Microsc. (Oxf.)*. 111:39–49.
18. Shuman, H., A. V. Somlyo, and A. P. Somlyo, 1976. Quantitative electron probe microanalysis of biological thin sections: method and validity. *Ultramicroscopy*. 1:317–339.
19. Somlyo, A V., H. Shuman, and A. P. Somlyo. 1977. Elemental distribution in striated muscle and effects of hypertonicity. Electron probe analysis of cryosections. *J. Cell Biol.* 74:828–857.
20. Statham, P. J. 1978. Quantitative chemical analysis with EDS systems. *In* Microbeam Analysis Society Proceedings Thirteenth Annual Conference. K. F. J. Heinrich, editor. Microbeam Analysis Society. National Bureau of Standards, Washington, D. C. T2A–T2L.
21. Sumner, A. T. 1978. Quantitation in biological x-ray microanalysis with particular reference to histochemistry. *J. Microsc. (Oxf.)*. 114:19–30.
22. Thornburg, W., and P. E. Mengers. 1947. An analysis of frozen section techniques: I. Sectioning of fresh-frozen tissue. *J. Histochem. Cytochem.* 5:47–52.
23. Yakowitz, H. 1975. Methods of quantitative x-ray analysis used in electron probe microanalysis and scanning electron microscopy. *In* Practical Scanning Electron Microscopy. J. I. Goldstein and H. Yakowitz, editors. Plenum Press, New York. 327–372.